

# Development and Preliminary Testing of Temporally Controllable Weather Modification Rocket with Spatial Seeding Capacity

Xiaobo Dong<sup>1,2,3,4</sup>, Xiaoqing Wang<sup>3</sup>, Yongde Liu<sup>5</sup>, Xiaorong Wang<sup>5</sup>

<sup>1</sup>China Meteorological Administration Xiong'an Atmospheric Boundary Layer Key Laboratory, Xiong'an New Area, 071800, China

<sup>2</sup>Key Laboratory of Meteorology and Ecological Environment of Hebei Province, Shijiazhuang, 050021, China

<sup>3</sup>Hebei Provincial Weather Modification Center, Shijiazhuang, 050020, China

<sup>4</sup>Xingtai Atmospheric Environment Field Scientific Test Base of CMA, 054200, China

<sup>5</sup>Xi'an Qinghua Commercial Explosives Corp., Ltd., Xi'an, 710025, China

*Correspondence to:* Xiaobo Dong (dongxiaobo@hebwmo.cn)

**Abstract.** Current weather modification rockets with a single operation mode, limited operating height, and fixed and uncontrollable operating time, cannot achieve seeding in different layers, stages and quantities for different cloud systems. Therefore, a temporally controllable weather modification rocket with spatial seeding capability is developed in this study. This new rocket features an electronic fuse-controlled intelligent ignition system, with eight channels of ignition tube outputs. Additionally, carrier wave communication technology is incorporated to set the seeding time for eight sets of ignition tubes. The temporally controllable rocket is capable of initiating seeding within 2–26 s and can conduct operations for layering, arbitrary altitude and fractional-dose seeding within the altitude range of 500–5500 m (at a launch angle of 70°), which is calculated based on the flight trajectory of rockets. The minimum time interval of the rocket for seeding can be set to 0.1 s, and all 48 catalyst bullets loaded in a single rocket can be launched within 0.8 s. Thus, the rocket can achieve both concentrated and continuous seeding. Consequently, during weather modification operations, the parameters such as altitude, thickness and operating temperature of target clouds can be obtained through detection, and they can be used to automatically calculate the suitable seeding time, seeding altitude and seeding dose by the launch control system based on the flight trajectory of rockets, so as to improve the accuracy and scientificity of cloud catalytic operations. Ground tests show that the reliabilities of the electric ignition tube output, new electronic fuse input and output, and electronic fuse output energy all meet the design specification. The temporally controllable spatial-seeding rocket can achieve adjustable and controllable seeding times for catalytic bullets, meeting the safety and reliability requirements of rockets.

29 **Keywords:** Temporally controllable; Weather modification; Spatial seeding rockets; Cloud seeding

## 30 **1 Introduction**

31 Weather modification primarily involves the dispersal of a certain amount of seeding agents such as silver iodide  
32 and dry ice into clouds at appropriate locations under conducive weather conditions using various tools such as  
33 aircraft, anti-aircraft guns, rockets and ground generators, in order to achieve artificial rainfall (snow), hail  
34 suppression and fog dispersal (Bruitjes, 1999; Mao and Zheng, 2006). Currently, silver iodide is the main catalyst  
35 used for cold cloud seeding operations. The quantity of effective ice nuclei produced during cold cloud seeding is  
36 related to the ambient temperature. Experimental results have demonstrated that the nucleation rate is the highest  
37 when the temperature of clouds ranges from  $-20\text{ }^{\circ}\text{C}$  to  $-4\text{ }^{\circ}\text{C}$ . Moreover, the ideal temperature range is between  
38  $-12\text{ }^{\circ}\text{C}$  and  $-5\text{ }^{\circ}\text{C}$ , where silver iodide exhibits the optimal ice nucleation effects (Lou et al., 2021).

39 With advancements in cloud and precipitation detection technology, research on the structure of target clouds for  
40 weather modification has become increasingly sophisticated, leading to improved accuracy in identifying  
41 operational conditions and locations. Aircraft-based precipitation enhancement operations can penetrate stratiform  
42 clouds, detect cloud microphysical characteristics, identify suitable seeding areas and conduct scientifically precise  
43 operations (Guo et al., 2021). However, during severe convective weather, aircraft operations are not feasible.  
44 Moreover, for widespread stratiform precipitating cloud systems, aircraft operations are constrained by factors such  
45 as flight range, flight time, and seeding dosage, limiting coverage of the entire operational area. Ground-based  
46 weather modification rocket operations can circumvent threats posed by high-altitude conditions and are suitable  
47 for situations where aircraft operations are challenging. Additionally, rocket operations in weather modification can  
48 complement aircraft operations to expand seeding coverage and improve seeding efficiency.

49 In northern China, the microphysical mechanisms of catalyzing stratiform clouds for artificial rainfall mainly  
50 involve the coordination of seeding clouds in the upper levels and feeder clouds in the lower levels to form  
51 precipitation. Seeding and feeder clouds are often governed by different dynamic conditions, and sometimes, they  
52 are not continuous cloud bodies, with occasional dry layers of different thicknesses between them (Yao, 2006; Hong  
53 and Lei, 2012; Dong et al., 2022). In hail suppression operations, it is desired that seeding agents be concentrated  
54 near the "funnel" of hail clouds (Xu, 2001; Xu and Tian, 2008; Yao et al., 2022). Observation results of stratiform  
55 clouds for winter snowfall in northern China from 2017 to 2022 indicated that winter stratiform clouds for snowfall  
56 exhibit more stability in development than spring and autumn stratiform precipitating clouds, with less fluctuations  
57 in cloud top height (mostly lower than 3500 m) (Dong et al., 2020, 2021; Liu et al., 2021; Fu et al., 2023; Wang et

58 al., 2023; Yan et al., 2023). In operations, the seeding height of most weather modification rockets is within 3–6  
59 km.

60 Currently, rocket seeding techniques in weather modification are categorized into line seeding and spatial seeding  
61 modes (Wang et al., 2018). Line seeding rockets have fixed seeding start times set at the time of production, and the  
62 seeding height varies mainly with the launch angles of the rocket launcher, with a relatively limited adjustable  
63 range of seeding altitudes. At present, the commonly used line seeding rocket has a seeding time of 15–30 s and a  
64 maximum launch altitude of 6000–8000 m. After the rocket is launched, the catalyst burns inside the rocket body  
65 and spreads along the direction of the rocket's flight trajectory. After seeding, a long linear silver iodide aerosol  
66 band is formed in the air. For spatial seeding rockets, although the start seeding time can be set before launch, the  
67 adjustment range is currently limited to 3–12 s. With a launch angle of 55°, the start seeding height is  
68 approximately between 2000 m and 3200 m, and seeding operations cannot be interrupted after starting. These two  
69 techniques carry out seeding operations on variable clouds with fixed settings in rockets. Thus, there are several  
70 phenomena, i.e., the temperature in the seeding position does not reach the effective temperature range of silver  
71 iodide, the seeding occurs in dry layers of stratiform clouds, and there is empty seeding (the seeding location is  
72 above cloud tops in winter).

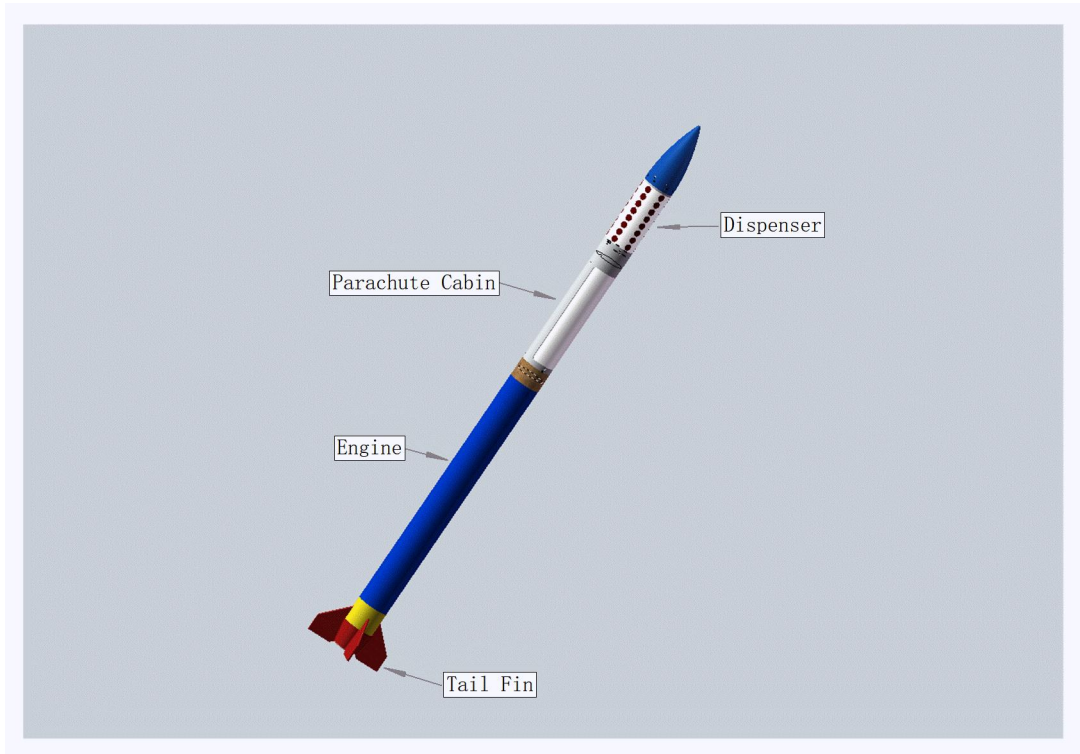
73 To address the above challenges, this study aims to develop a new generation of weather modification rockets with  
74 temporally controllable and adjustable seeding capabilities. By presetting accurate seeding start times, quantities  
75 and end times before rocket launch based on the actual height and thickness of clouds at the operational site, these  
76 rockets can enter target clouds and conduct operations according to the preset seeding parameters, thereby  
77 improving the scientific and the precision of weather modification rockets for precipitation enhancement and hail  
78 suppression.

79 The remainder of this paper is arranged as follows. Section 2 introduces the principles of spatial-seeding rockets for  
80 weather modification. Section 3 discusses the principles of the spatial-seeding rocket with a temporally controllable  
81 ability. The ground testing results for temporally controllable spatial-seeding rockets are analyzed in sec. 4. Section  
82 5 investigates the safety of temporally controllable spatial-seeding rockets. The main conclusions are presented in  
83 sect. 6.

## 84 **2. Principles of spatial-seeding rockets for weather modification**

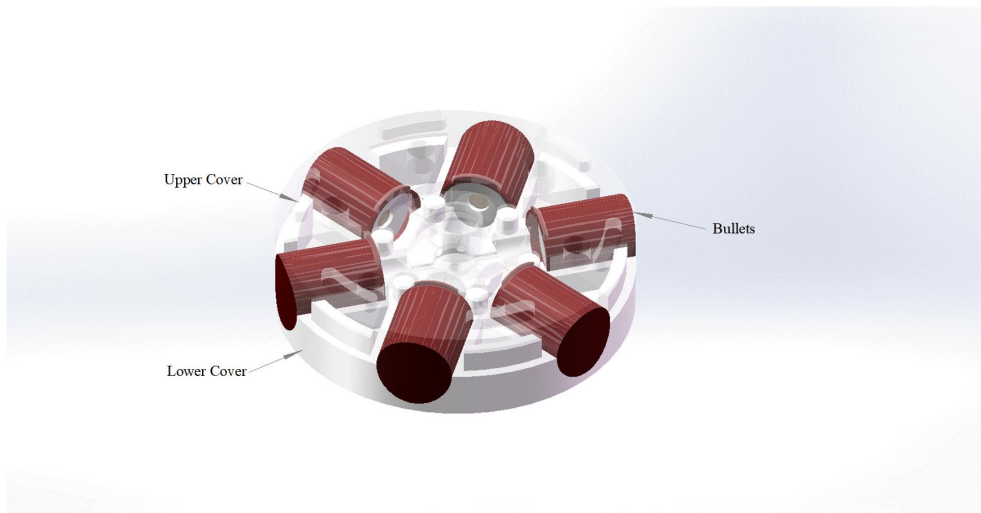
85 The technology of spatial-seeding rockets for weather modification is derived from the concept of submunition, i.e.,

86 the internal ejection mechanism generates power to disperse submunitions from cluster munition upon reaching the  
87 target, thus improving the utilization efficiency of ammunition. For instance, the projectile of the ZBZ-HJ-7  
88 spatial-seeding rocket consists of a dispenser, a safety landing system (parachute cabin), an engine and a tail fin  
89 (Fig. 1). The rocket has a diameter of 82 mm, a length of 1660 mm and a weight of 10.8 kg.



90  
91 **Figure 1: Schematic diagram of the ZBZ-HJ-7 spatial-seeding rocket.**  
92

93 The dispenser consists of one wind cap, eight sets of launch modules, one control cabin and one electronic fuse.  
94 Each set of launch modules consists of an upper cover, a lower cover, six bullets filled with catalysts, and one delay  
95 ignition tube. The structure diagram of a single launch module is shown in Fig. 2.



96

**Figure 2: Structure diagram of a single launch module.**

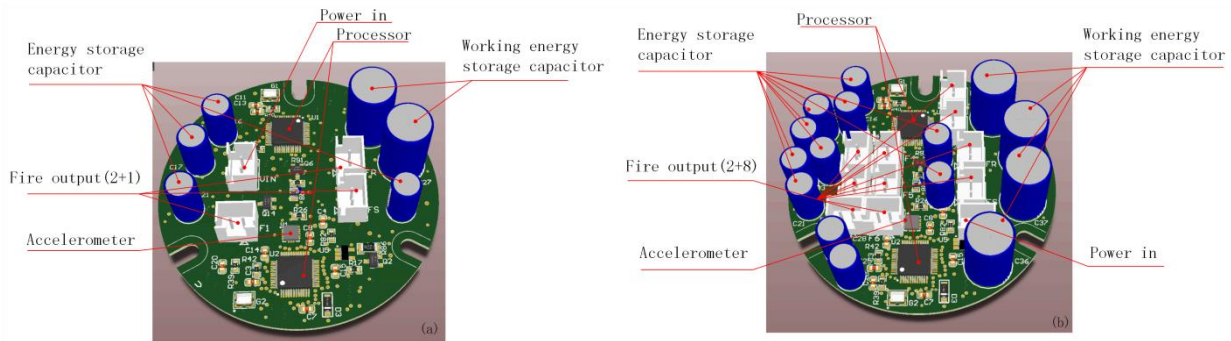
97  
98  
99 The main difference between spatial-seeding rockets and line-seeding rockets lies in the structure of the warhead  
100 charge. For line-seeding rockets, a catalyst charge column is assembled in the warhead. When the charge column is  
101 ignited from the end face, the combustion products are dispersed outward along the trajectory through small holes  
102 on the side of the projectile body. In contrast, in terms of spatial-seeding rockets, the catalytic material is packed  
103 into the bullets, which are vertically mounted along the projectile axis inside the warhead cylinder. A delay ignition  
104 tube matching the catalyst bullets is installed in the center of the projectile axis. After the rocket is launched, the  
105 delay ignition tube will be ignited at the setting time, thereby igniting the surrounding catalyst bullets. Then, the  
106 propellant inside the catalyst bullets will propel them out of the projectile body and ignite the catalyst inside the  
107 bullets simultaneously. The high temperature generated by combustion causes silver iodide crystals and other  
108 substances in the catalyst to sublime into silver iodide aerosol.

109 The ZBZ-HJ-7 spatial-seeding rocket carries a total of 48 catalyst bullets, arranged in eight rows along the rocket  
110 axis, with six bullets per row. After the rocket is launched, the electronic fuse starts timing, and after reaching the  
111 seeding time (preset before launching), the electronic fuse ignites the delay ignition tube in the first set of launch  
112 modules. After a delay of 2.7 s, the delay ignition tube ignites the six catalyst bullets in the first set of launch  
113 modules, which exit the cabin at a speed of  $\geq 40 \text{ m}\cdot\text{s}^{-1}$ . Simultaneously, the delay ignition tube in the second set of  
114 launch modules is ignited. After another delay of 2.7 s, the six catalyst bullets in the second set of launch modules  
115 are ignited. In this way, all eight sets of launch modules are fired. Near the apex of the flight trajectory, the  
116 spatial-seeding rocket deploys a parachute, and the debris descends slowly. Each catalyst bullet carries 6.2 g of  
117 silver iodide. The combustion of the catalyst bullets forms a silver iodide aerosol band in the space they traverse.  
118 The flight trajectory of the bullets is perpendicular to that of the rocket, with a flight distance of at least 200 m.  
119 After all the bullets for precipitation enhancement are dispersed from the projectile body, an instantaneous catalytic  
120 zone with a diffusion cross-section diameter of approximately 500 m and a length of 6.6 km is formed in space.

### 121 **3. Principles of temporally controllable spatial-seeding rockets**

122 To achieve precise seeding for target clouds at different heights and thicknesses, as well as multi-layer cloud  
123 systems, a comprehensive analysis and design improvement are conducted on the ZBZ-HJ-7 spatial-seeding rocket.  
124 The aim is to ensure that each layer of launch modules disperses according to the flight trajectory (time), replacing  
125 the original design scheme of fixed-delay ignition tubes with a new sequential ignition design controlled by

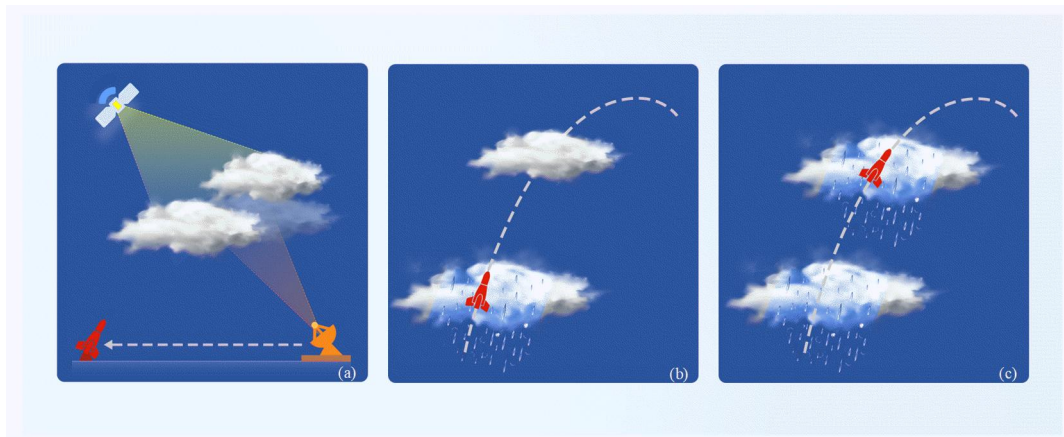
126 electronic fuses. Seven ignition outputs are added to this new design scheme. The start seeding time of the rocket  
 127 can be set within 2–26 s, corresponding to a range of start seeding heights within 500–5,500 m (at a launch angle of  
 128 70°). The minimum seeding time interval can be set to 0.1 s, allowing all 48 catalyst bullets carried by a single  
 129 rocket to be launched within 0.8 s. To realize these improvements, four designs are made for the rocket. Firstly,  
 130 electric ignition tubes are installed in the launch modules, requiring structural and circuitry redesign. Secondly, the  
 131 electronic fuse outputs increase from one to eight, and the electrical interface is redesigned (Fig. 3). Additionally,  
 132 changes are made to the parameters received by the electronic fuse and the data output, requiring the redesign of  
 133 parameter binding methods and software. Finally, the functions of the electronic fuse and the dispenser are largely  
 134 altered, and the testing and inspection methods are redesigned.



135  
 136 **Figure 3: Three-dimensional model diagrams of the electronic fuses of (a) the ZBZ-HJ-7 spatial-seeding rocket and (b)**  
 137 **the temporally controllable spatial-seeding rocket.**

138  
 139 The operational design of temporally controllable spatial-seeding rockets is outlined as follows. Before weather  
 140 modification operations, the multi-source observation data are integrated and analyzed to obtain the parameters  
 141 suitable to target clouds, such as the number of cloud layers, cloud base height and cloud thickness. These  
 142 parameters are input into the launch control system along with launch parameters (local altitude and launch angle).  
 143 Then, the launch control system automatically calculates the seeding time of eight sets for target clouds based on  
 144 the flight trajectory of rockets (Fig. 4a). Afterwards, the seeding time of eight sets is automatically loaded into  
 145 rockets by using carrier wave communication technology. The two contacts on rockets are connected to the launch  
 146 control system through wires on the launching rack. The launch control system applies electrical signals with a  
 147 specific frequency to the two contacts, which are demodulated by the electronic fuse to set the seeding times  
 148 correctly.  
 149 The rocket begins timing from the moment of lifting off the launching rack. At each set seeding time point, six  
 150 catalyst bullets in each row are ejected. For example, assume that the target cloud system has two layers, with the  
 151 lower layer in heights of 1000–3000 m and the upper layer in heights of 4000–4500 m. As the lower layer is thicker

152 and the upper layer is thinner, the seeding dosage can be set to five rows of bullets for the lower layer and three  
153 rows for the upper layer. If the launch angle is  $65^\circ$ , the theoretical calculation indicates that the seeding operation of  
154 the rocket begins after 2.6 s in the first layer, at an approximate height of 1,200 m. The time interval between the  
155 ejections of each set of bullets is 1 s, and the seeding is completed after 5 s (Fig. 4b), at which time the altitude of  
156 the rocket is approximately 2800 m. The dispersion in the second layer begins after 12.3 s, at an altitude of  
157 approximately 4,200 m. Since the thickness of the cloud layer is only 500 m, and the flight speed of the rocket  
158 decreases when reaching a high altitude, the seeding interval can be set to 0.2 s, thus achieving the goal of  
159 concentrated seeding within a thinner cloud layer (Fig. 4c).



160  
161 **Figure 4: Schematic diagram of the working demo of a temporally controllable spatial-seeding rocket.**

#### 162 **4. Ground testing result analysis for a temporally controllable spatial seeding rocket**

163 A temporally controllable spatial-seeding rocket is deeply improved and developed on the basis of the ZBZ-HJ-7  
164 spatial-seeding rocket. According to the requirements of engineering design, it is necessary to conduct  
165 comprehensive ground tests and experiments to verify the feasibility and reliability of the new technical state. The  
166 ground tests primarily consist of three main parts: reliability tests of the electric ignition tube outputs, the new  
167 electronic fuse input and output, and the output energy of the new electronic fuse.

##### 168 **4.1 Reliability test of electric ignition tube outputs**

169 One major improvement in temporally controllable spatial-seeding rockets is the replacement of the electric ignition  
170 tubes with the original ignition tube with a fixed delay of 2.7 s. The electric ignition tubes mainly consist of a  
171 bridge wire, igniting powder and lead wires. The igniting powder tightly encases the bridge wire, and when current  
172 passes through the bridge wire, heat is generated according to Joule's law ( $Q = I^2 \cdot R \cdot t$ ). The bridge wire is highly

173 sensitive to heat, and when heat is generated, the temperature of the bridge wire instantly rises. When the  
174 temperature reaches the ignition temperature of igniting powder, igniting powder ignites, producing  
175 high-temperature gas and hot metal particles to ignite the initiating explosive device of the next stage. Temporally  
176 controllable spatial-seeding rockets prioritize the use of matured standardized No. 32 electric ignition tubes as  
177 ignition components. These tubes have an ignition compound weight of 18–22 mg, ensuring stable and reliable  
178 ignition outputs.

179 In order to test the reliability of electric ignition tubes to ignite catalyst bullets in the launch module, a dispenser  
180 assembled with eight sets of launch modules, each equipped with one electric ignition tube, is designed. One set of  
181 electric ignition tubes is randomly selected to input igniting energy, and the ignition status of catalyst bullets in this  
182 set is observed. A total of eight sets of launch modules, namely eight electric ignition tubes, are tested, igniting a  
183 total of 48 catalyst bullets. The test results show that after the electric ignition tubes work, all six catalyst bullets in  
184 each set of launch modules are ignited. The catalyst bullets fly out of the launch modules at high speed and burn  
185 stably during the flight, and their burning time meets the technical specifications. The proper functioning of electric  
186 ignition tubes determines whether the dispenser can operate effectively, which is critical in the entire ignition. To  
187 ensure the reliability of the electric ignition tubes to ignite catalyst bullets, in the formal design of the dispenser,  
188 two electric ignition tubes are installed in each set of launch modules as backups for each other. Hence, tests are  
189 conducted with eight sets of launch modules, each equipped with two electric ignition tubes, totaling 16 electric  
190 ignition tubes and 48 catalyst bullets. All tested catalyst bullets fly and burn normally after the electric ignition  
191 tubes are activated.

#### 192 **4.2 Reliability test of the input and output of the new electronic fuses**

193 To test the accuracy and reliability of the output timing sequence of the new electronic fuse, a dedicated upper  
194 computer software for the electronic fuse is designed. A seeding time calculation program is developed, and an  
195 output signal acquisition system is constructed. The testing methods are as follows. Firstly, the cloud parameters  
196 and launch angles are input into the seeding time calculation program to calculate eight sets of seeding time points  
197 and the optimal parachute opening time. Subsequently, the eight sets of seeding times and parachute opening times  
198 are loaded into the electronic fuse through the dedicated upper computer. Finally, the signal acquisition system is  
199 docked with the electronic fuse. After the electronic fuse is powered on, the signal acquisition system automatically  
200 records the output time of the timing controller. Table 1 shows the test results of one of the electronic fuses.

201 After repeated tests on ten electronic fuses, the cumulative valid data records are over 4,800. The test results show



202 that the deviation between the actual output time and the loaded time is within  $\pm 0.1$  s, indicating that the electronic  
 203 fuses output accurate seeding time points and are reliable.

204

205 **Table 1. Test results of an electronic fuse for seeding time: loaded and actual output.**

Serial number		Parachute opening time (s)	Seeding time (s)							
1	Load time	28.9	3.1	3.8	4.6	5.3	10.4	12.3	14.2	16.1
	Observed time	28.8	2.9	3.7	4.4	5.1	10.2	12.1	14.1	15.9
		28.8	2.9	3.7	4.4	5.1	10.3	12.1	14.1	15.9
		28.9	3.2	3.8	4.5	5.2	10.5	12.2	14.2	16.0
		29.1	3.1	3.8	4.6	5.3	10.4	12.4	14.2	16.1
2	Load time	30.4	64	103	142	181	220	259	289	337
	Observed time	30.2	63.9	102.8	141.9	180.9	220	258.8	288.8	336.8
		30.3	63.9	102.8	141.8	180.8	218.8	258.8	288.9	337.2
		30.4	63.9	102.9	141.9	180.9	220	259	289.0	336.9
		30.3	63.9	102.9	141.8	180.9	219.9	258.9	289.2	336.9
3	Load time	50	100	150	200	250	300	350	400	450
	Observed time	49.8	99.8	149.9	199.9	249.8	299.8	349.9	399.8	449.8

206 Note: Serial number 3 indicates the operational capability of the timing controller under extreme conditions.

207 **4.3 Reliability test of the output energy of the new electronic fuses**

208 The prerequisite for electric ignition tubes to ignite is that the energy input by electronic fuses must be greater than  
 209 the critical igniting energy of electric ignition tubes. In other words, the output energy of electronic fuses  
 210 determines the reliability of igniting electric ignition tubes. The most efficient way for the electronic fuses to output  
 211 igniting energy is by discharging the capacitor ( $Q = 0.5 \cdot C \cdot U^2$ , where Q denotes the output energy, C the  
 212 capacitance, and U the voltage across the capacitor). In engineering practice, a fixed capacitance capacity is often  
 213 used, and the voltage across the capacitor is adjusted to test whether the output energy can ignite the corresponding  
 214 initiating explosive devices.

215 In this research, in order to verify whether the new electronic fuses can reliably ignite the electric ignition tubes in  
 216 the launch modules, a set of sensitivity tests is conducted on the new electronic fuses following the method  
 217 specified in *The up-and-down estimate method for sensitivity test* (Standard No.: GJB 377–1987). With the

218 capacitance kept constant, a set of sensitivity tests is performed with the capacitor discharge voltage as the variable.  
219 Based on the 32 valid data accumulated in the test and the equation  $Q = 0.5 \cdot C \cdot U^2$ , we can calculate that the  
220 igniting reliability can achieve 99.99% when the capacitance capacity (C) is 220  $\mu\text{F}$  and the capacitor voltage (U) is  
221 11 V, which meets the critical energy for reliable ignition of electric ignition tubes.

222 Subsequently, the new electronic fuse undergoes a test for its maximum operating time. At its maximum possible  
223 operating time, the output capacitor voltage is measured not to be lower than 16 V, suggesting that the actual output  
224 energy of electronic fuses is approximately 2.1 times higher than the critical igniting energy for electric ignition  
225 tubes (with a capacitor voltage U of 11 V), which meets the general design requirements for a pyrotechnic sequence  
226 with a 2-fold ignition margin.

227 After the output igniting energy of new electronic fuses is decided to be sufficient, an output reliability test for new  
228 electronic fuses is conducted. Each new electronic fuse initiates eight sets of dual electric ignition tubes, and a total  
229 of 80 tubes are ignited by ten electronic fuses. All electric ignition tubes ignite normally, and the ignition time  
230 points are consistent with the loaded time points. The test results suggest that the electronic fuses can reliably ignite  
231 electric ignition tubes in ground tests.

#### 232 **4.4 Ground tests of dispenser**

233 Based on the tests of individual subsystems above, two sets of dispensers are assembled for ground seeding and  
234 flight distance testing of catalyst bullets in formal operational status to assess the overall performance of the  
235 improved dispensers. The two sets of dispensers are powered on and initiated according to the load times of serial  
236 numbers 1 and 2 in Table 1. The results reveal that all 96 catalyst bullets are launched from the launchers at the  
237 preset time. The catalyst bullets burn normally, and the flight distances meet the technical requirements. These  
238 findings indicate that improved temporally controllable spatial-seeding rockets meet the design requirements and  
239 achieve controllable and accurate seeding.

#### 240 **5. Safety of temporally controllable spatial seeding rockets**

241 Based on the ZBZ-HJ-7 rocket, a temporally controllable spatial-seeding rocket improves the igniting sequence of  
242 the dispenser. Since the structure of the rocket body is the same as that of the original rocket, the trajectory and  
243 safety program also remain unchanged. The main technical specifications of temporally controllable rockets and the  
244 ZBZ-HJ-7 spatial-seeding rocket are listed in Table 2. The seeding time of the total bullets has been changed from  
245  $\geq 27$  s to 0.8–32 s, which reflects the adjustable and controllable ejection height and duration of the temporally

246 controllable spatial-seeding rocket. The load time range of electronic fuses has been changed from 6–17 s to 2–26 s,  
 247 expanding the range of new rocket seeding heights. The seeding time interval of electronic fuses has been changed  
 248 from the original fixed 2.7 s to 0.1–26 s, which can achieve continuous and concentrated seeding.

249  
 250 **Table 2. Main technical specifications of the temporally controllable spatial-seeding rockets and the**  
 251 **ZBZ-HJ-7 spatial-seeding rocket.**

Technical specifications	ZBZ-HJ-7 rocket	Temporally controllable rocket
Rocket diameter (mm)	82	82
Bullet length (mm)	1660	1660
Bullet weight (kg)	10.8	10.8
Maximum launch height (m)	≥7000 (85°)	≥7000 (85°)
Number of catalyst bullets (rounds)	48	48
Total amount of silver iodide carried by catalyst bullets (g)	≥20	≥20
Nucleation rate of silver iodide at -10°C (pcs/g)	≥1.18×10 <sup>14</sup>	≥1.18×10 <sup>14</sup>
Lateral flight speed of single bullets (m/s)	≥40	≥40
Burning time of single bullets (s)	6–9	6–9
Seeding time of the total bullets (s)	≥27	0.8–32
Load time range of electronic fuses (s)	6–17	2–26
Seeding time interval of electronic fuses (s)	2.7	0.1–26
Landing speed of debris (m/s)	≤8	≤8

252  
 253 During the long storage validity period, the rocket body is sealed, and the internal propellant is designed to  
 254 withstand the environment within -30°C to 50°C. Temperature and humidity variations can not decrease the safety  
 255 of rocket body. After loading onto the launching rack and before being powered on, the internal initiating explosive  
 256 devices of rockets are all semi-insensitive, with a safety current level higher than that of common civilian initiating  
 257 explosive devices, which can withstand general stray current shocks and possess a higher ability to resist accidental  
 258 electrical stimulation. During the self-check and loading phase after powering on, the voltage in the electronic fuses  
 259 is at only 3.3 V, which even under extreme conditions does not trigger the internal ignition sequence. Upon pressing  
 260 the launch button, the electronic fuses charge to a working voltage of 24 V within 1 s. Once detecting that the  
 261 capacitor voltage exceeds the critical value, the electronic fuses immediately ignite the engine. Subsequently, the

262 rocket leaves the launching rack at high speed, and electronic fuses start timing. Any lapse or failure in the  
263 aforementioned process prompts an immediate internal discharge program. In an extreme case, if the engine ignites  
264 but the propellant fails to burn, the rocket does not leave the launching rack and the attitude sensor in the electronic  
265 fuse does not receive a flight signal. In this situation, all the energy stored in the capacitors of electronic fuses will  
266 be discharged within 3 s to ensure that the rocket will not seed or deploy its parachute on the launching rack, thus  
267 remaining in a safe and unpowered state for subsequent handling.

268 The new design sets the operation time for rockets by using carrier wave communication technology. The input  
269 signal must pass through a demodulation program, and until the input signal is demodulated, the electronic fuses  
270 consider any input signals as invalid. Directly applying launch energy or other forms of energy, electronic fuses will  
271 not activate the working program. This design eliminates the safety risk of the rocket launching as soon as it is  
272 powered on. The parachute deployment mechanism, which reliably operates near the apex of the trajectory, has  
273 been used over 50,000 instances in the ZBZ-HJ-7 rocket, demonstrating its reliability.

## 274 **6. Conclusions**

275 In order to achieve precise, timed and quantified seeding operations of weather modification rockets, the temporally  
276 controllable spatial-seeding rocket is developed by redesigning the ignition control unit and improving the  
277 operational parameters loading method. During seeding operations, parameters such as cloud height, thickness and  
278 operating temperature can be automatically calculated by using detected data. Based on these parameters, the  
279 appropriate seeding time points, heights and dosages can be determined, thus enhancing the precision and  
280 scientificity of cloud seeding operations. The main conclusions are as follows.

281 The newly designed temporally controllable spatial-seeding rocket replaces the fixed-delay ignition with intelligent  
282 ignition controlled by electronic fuses, with eight-channel electric ignition tubes. Additionally, carrier wave  
283 communication technology is used to set operational parameters, which enable the rocket to have functions such as  
284 adjustable and controllable time sequences for seeding operations. The seeding start time of rockets can be set as  
285 2–26 s, and the seeding height varies in the range of 500–5500 m (at a launch angle of 70°). Within this range,  
286 seeding operations can be carried out at different altitudes and dosages. The minimum seeding time interval can be  
287 set to 0.1 s, enabling all 48 catalyst bullets to be launched within 0.8 s, thereby achieving both continuous and  
288 concentrated seeding.

289 Ground tests are conducted on the temporally controllable spatial-seeding rocket, including reliability tests of

290 electric ignition tube output, new electronic fuse input and output, and electronic fuse output energy. The results  
291 indicate that all 16 electric ignition tubes work reliably, and 48 catalyst bullets launch and ignite normally. Over  
292 4,800 valid data points are collected during repeated testing of ten electronic fuses. The deviation between the  
293 actual output time of the electronic fuses and the set time is no more than  $\pm 0.1$  s. Additionally, all 80 electric  
294 ignition tubes are successfully ignited. Based on preliminary testing, ground tests are conducted on the dispenser.  
295 All the 96 catalyst bullets are dispersed according to the present time and burn normally. The improved temporally  
296 controllable spatial-seeding rocket meets design requirements, achieving controllable and precise seeding.  
297 The temporally controllable spatial-seeding rocket is based on the structure of the ZBZ-HJ-7 spatial-seeding rocket,  
298 with improvements limited to the dispenser, while the engine and parachute compartment remain unchanged. In  
299 addition, the aerodynamic shape, mass center and thrust of the rocket remain unaltered, and thus, the ballistic  
300 trajectory is the same as that of the original design. The use of carrier wave communication technology eliminates  
301 the safety risk of rocket launching as soon as it is powered on, ensuring the safety and reliability of the rocket.  
302 Based on the insights in this study, future research will involve observation and catalyst experimental design and  
303 carry out catalyst tests for different precipitating cloud systems in northern China by using temporally controllable  
304 spatial-seeding rockets. Moreover, Experiment data will be accumulated, and physical tests of the effects of cold  
305 cloud seeding operations will be conducted to verify the actual effects of the new seeding rocket.

306

### 307 ***Author contributions***

308 Xiaobo Dong provided methods and ideas for the temporally controllable spatial-seeding rocket. The experiments  
309 were designed by Yongde Liu and Xiaorong Wang. Xiaobo Dong wrote the first draft, which was further revised by  
310 Yongde Liu and Xiaoqing Wang.

### 311 ***Competing interests***

312 The authors declare that they have no conflict of interest.

### 313 ***Disclaimer***

314 Publisher's note: Copernicus Publications remains neutral with regard to jurisdictional claims made in the text,  
315 published maps, institutional affiliations, or any other geographical representation in this paper. While Copernicus  
316 Publications makes every effort to include appropriate place names, the final responsibility lies with the authors.

### 317 ***Acknowledgement***

318 This work was supported by Hebei Natural Science Foundation ( D2023304001 ) and China Meteorological  
319 Administration Innovation and Development Project(CXFZ2023J038).We thank Nanjing Hurricane Translation for

320 reviewing the English language quality of this paper.

321 **References**

322 Bruintjes, R. T.: A review of cloud seeding experiments to enhance precipitation and some new prospects, 1999.

323 Dong, X. B., Zhao, C. F., Yang, Y., et al.: Distinct change of supercooled liquid cloud properties by aerosols from  
324 an aircraft-based seeding experiment, *Earth and Space Sci.*, 7,e2020EA001196.

325 <https://doi.org/10.1029/2020EA001196>, 2020.

326 Dong, X. B., Zhao, C. F., Huang, Z. C., et al.: Increase of precipitation by cloud seeding observed from a case study  
327 in November 2020 over Shijiazhuang, China, *Atmospheric Res.*, 262,105766.

328 <https://doi.org/10.1016/j.atmosres.2021.105766>, 2021.

329 Dong, X. B., Sun, X. S., Yan, F., et al.: Aircraft Observation of a Two-Layer Cloud and the Analysis of Cold Cloud  
330 Seeding Effect, *Front. Environ. Sci.*, 10:855813, 2022.

331 Fu, J., Zhang, D., Dong, X. B., et al.: A Comparative analysis of microphysical structure of snowfall cloud system  
332 in central and southern Hebei based on aircraft observation, *Desert and Oasis Meteorology*,17(5):64-70, 2023.

333 Guo, X. L., Fu, D. H., Guo, X., et al.: Advances in aircraft measurements of clouds and precipitation in China. *J.*  
334 *Appl. Meteor. Sci.*, 32(6): 641-652, 2021.

335 Hong, Y. C., Lei, H. C.: Research advance and thinking of the cloud precipitation physics and weather modification,  
336 *Climatic and Environmental Research (in Chinese)*, 17(6): 951-967, 2021.

337 Liu, W., Sun, Y. W., Xie, X. Y., et al.: Analysis of the structure characteristics and seeding possibility of stratiform  
338 clouds with low cold front in Hebei Province in winter, *Journal of Meteorology and Environment*, 37(3),110-116,  
339 2021.

340 Lou, X. F., Fu, Y., Su, Z. J.: Advances of silver iodide seeding agents for weather modification, *J. Appl. Meteor.*  
341 *Sci.*, 32(2): 146-159, 2021.

342 Mao, J. T., Zheng, G. G.: Discussions on weather modification issues, *Journal of Applied Meteorological*  
343 *Science(in Chinese)*, 17(5): 643-646, 2006.

344 Wang, W. T., Jia, S., Wang, D. W., et al.: Comparative study in catalyst seeding technology of rocket for rain  
345 enhancement or hail suppression, *Advances in Meteorological Science and Technological*, 8(6): 95-101, 2018.

346 Wang, X. Q., Dong, X. B., Yan, F., et al.: A comprehensive observational study of micro-physical evolution  
347 characteristics of a snowfall cloud system under winter cold front in Hebei Province, *Meteorological Science and*  
348 *Technology*, 51(2):233~244, 2023.

349 Yan, F., Yang, J. F., Dong, X. B., et al.: Airborne Observations of the Cloud Vertical Microphysical Characteristics  
350 of Warm Conveyor Belt within a Winter Mesoscale Snowstorm, *Chinese Journal of Atmospheric Sciences* (in  
351 Chinese), 47(5): 1451–1465 doi:10.3878/j.issn.1006-9895.2203.21180, 2023.

352 Yao, Z. Y.: Review of weather modification research in Chinese Academy of Meteorological Sciences, *J. Appl.*  
353 *Meteor. Sci.*, 17(6): 786-795, 2006.

354 Yao, Z. Y., Tu, Q., An, L., et al.: Review of advances in hail formation process and hail suppression research, *Acta*  
355 *Meteorological Sinica*, 80(6): 835-863 (in Chinese), 2022.

356 Xu, H. B.: The possible dynamic mechanism of explosion in hail suppression, *Acta Meteor Sinica*, 59(1): 66-76 (in  
357 Chinese), 2001.

358 Xu H B, Tian L Q.: Physical meanings of “cave channel” in strong convective storm with its application. *J Appl*  
359 *Meteor Sci*, 19(3): 372-379 (in Chinese). 2008.